JOURNAL OF MATERIALS SCIENCE MATERIALS IN MEDICINE 4 (1993) 117–126

Passive dissolution kinetics of titanium *in vitro*

K. E. HEALY*, P. DUCHEYNE
Department of Bioengineering, University of Pennsylvania, Philadelphia, PA 19104–6392, USA

The dissolution of titanium in simulated interstitial electrolyte (SIE), human serum in SIE (serum/SIE) and 8.0 mM ethylenediaminetetraacetic acid (EDTA) in SIE (EDTA/SIE) was measured *in vitro*. Titanium fibre samples were immersed in these solutions and maintained at 37 °C, 10% O_2, 5% CO_2 and 97 ± 3% relative humidity for 0–5000 h. The concentration of titanium released was quantified using electrothermal atomic absorption spectroscopy. Changes in oxide stoichiometry were determined by Auger electron spectroscopy after processing and immersion in the test solutions. The oxide became nearly stoichiometric TiO_2 after immersion, suggesting equilibration of the surface with the solutions. Solution ligands enhanced the magnitude of dissolution, with EDTA > serum/SIE > SIE. The dissolution kinetics were empirically fitted by a two-phase logarithmic relationship. The first phase of dissolution ($t < 300$ h) was dominated by equilibration of the oxide with the solution and the second phase ($t > 300$ h) by mass diffusion. The dissolution kinetics were similar for the EDTA/SIE and serum/SIE solutions, indicating that the mechanisms of dissolution for each solution may be the same.

1. Introduction

The favourable local tissue response to titanium has promoted its widespread use as an implant material. Titanium, however, is not inert when incorporated into the aggressive medium of the human body. Titanium releases corrosion products into the surrounding tissues and fluids [1–7]. However, the meaning of these results is unclear because of the absence of values for the standard concentration of titanium in body fluids and tissues [8, 9]. There is also no uniform conclusion of the role that biomolecules play on the corrosion rate. It was found that neither bovine albumin nor fibrinogen affected dissolution [10]. Furthermore, amino acid additions to Ringer's solution did not influence the corrosion rate [11]. On the contrary, polarization resistance experiments of titanium exposed to 10% calf serum in saline increased the corrosion rate by 31% compared with saline [12].

The composition, structure, thickness and, as a corollary, the conditions of preparation of the passive oxide film have been implicated in affecting passive dissolution rates [13]. Electrochemical studies on air-formed oxides in non-physiological electrolyte solutions have indicated that the native oxide formed was too thin to impart passivity to the metal, and that further thickening was necessary before passivity was achieved [14]. Evidence suggesting the importance of the passive layer in preventing corrosion can be inferred from an *in vitro* study which measured the release of titanium from samples with different surface conditions [15, 16]. A comparison of the amount of titanium released from passivated and non-passivated samples demonstrated a drastic increase in release rate for the latter. Furthermore, a different surface finish affected the rest potentials of titanium, where a higher potential, indicating a greater resistance to dissolution, was associated with smoother samples [11].

It is hypothesized that the physical chemical properties of the oxide and solution constituents such as serum biomolecules affect the dissolution kinetics of titanium. Determining the dissolution kinetics is a prerequisite for identifying the associated mechanisms that control the phenomenon *in vitro*, the knowledge of which represents a first step towards a further understanding of the biological performance of metallic materials. In light of this, the specific objectives of this study were to determine the effect of human serum on the passive dissolution kinetics of titanium samples with defined surface chemistry and to model, *in vitro*, the effect of solution ligands.

2. Materials and methods

2.1. Model solutions

The passive dissolution kinetics were identified for three solutions: physiological electrolytes without or with serum, and a solution simulating the later; SIE, human serum in SIE (serum/SIE) and 8.0 mM EDTA in SIE (EDTA/SIE). These solutions were chosen to vary the constituents thought to influence passive

* *Present address*: Division of Biological Materials, Northwestern University, 311 East Chicago Avenue, Chicago, IL 60611–3008, USA.

0957–4530

TABLE I Electrical equivalent concentration of electrolytes in various media

Substance	Serum [40] (mM)	SIE (mM)	Serum/SIE (mM)	EDTA/SIE (mM)
Na^+	152	152	152	168
K^+	5	5	5	5
Ca^{2+}	5	5	5	5
Mg^{2+}	3	3	3	3
Cl^-	113	135	121	135
HCO_3^-	27	27	27	27
HPO_4^{2-}	2	2	2	2
SO_4^{2-}	1	1	1	1
Proteins	16	0	9.6	16
pH	7.4	7.6	7.5	7.2

dissolution kinetics parametrically. SIE is a non-proteinaceous control that contains the electrolyte constituents of serum and interstitial fluid. The appropriate concentrations of electrolytes were determined by matching each to their corresponding electrical equivalence in serum. The milliequivalent concentrations of each electrolyte per litre water for serum, SIE, serum/SIE and EDTA/SIE are given in Table I.

The serum/SIE contained 60 vol % human serum and 40 vol % SIE. The percentage of serum used was based on the average subcutaneous interstitial fluid concentration of the proteins albumin and immunoglobulin G [17]. These proteins were chosen to represent the general protein concentration of interstitial fluid, which is similar to the fluid an implant confronts *in vivo* in the absence of inflammation.

A solution simulating the activity of serum used the chelating agent EDTA. The use of EDTA is based on the assumption that ions that are released from the metal surface *in vivo* do not remain in solution around the metal surface. Instead they form complex molecules and may be transported away through fluid motion. As a result a steady state of dissolution and reprecipitation is never achieved.. This divergence from the steady state is modelled by the complexing activity of EDTA. The efficacy of EDTA as a metal–complex chelating agent was verified by previous experiments, in which EDTA effectively reacted with released titanium and prevented it from being available for further reaction [18]. The chemical properties of EDTA make it a good choice to model the effect of proteins and biomolecules on dissolution kinetics. EDTA is a polyaminocarboxylic acid with six bonding sites, four carboxyl and two amino groups, available for bonding to metal cations in solution. These functional groups are similar to the domains on proteins postulated to be responsible for increasing the dissolution of titanium *in vivo*. This weak acid looses the carboxyl protons according to the following ionization equilibrium constants: $pK_1 = 2.0$; $pK_2 = 2.67$; $pK_3 = 6.16$ and $pK_4 = 10.26$ [19]. The pK-values indicate that at the pH of the EDTA/SIE solution (7.2), the ligand charge is either -2 or -3. The 8.0 mM EDTA reflects the electrical equivalent concentration of proteins in serum assuming the valence of the EDTA is -2. EDTA rapidly combines with metal cations in a 1:1 ratio regardless of the cation valency.

All reagents used to prepare the SIE and EDTA/SIE solutions were of the highest purity available (J. T. Baker, Ultrex grade, Phillipsburg, New Jersey; Aesar, Puratonic, Seabrook, New Hampshire). The metal salts used were NaCl, $NaHCO_3$, KCl, KH_2PO_4, $CaCl_2 \cdot 6H_2O$, $MgSO_4 \cdot 7H_2O$, $MgCl_2 \cdot 6H_2O$, Na_2HPO_4, disodium-EDTA ($Na_2EDTA \cdot H_2O$) and glucose.

Blood was collected from healthy males aged 25–40 years. Anticoagulants were not present in the collection bags, since the citrate components enhance the dissolution kinetics of titanium in a manner similar to EDTA [16, 20]. After the blood clotted it was spun in a centrifuge and the serum was withdrawn and proportioned to make 60:40 (by volume) serum to SIE. All solutions were filter-sterilized before use.

2.2. Sample fabrication

Titanium fibres (Bekaert NV, Zwevegem, Belgium) 20 mm in length and 0.05 mm in diameter were used to fabricate high surface area samples. During fabrication of the fibres iron may diffuse into the titanium surface. High levels of iron affects the electrochemical properties of titanium [21, 22], so the diffusion layer was removed by using an acid-etching protocol. A 25 g batch of fibres was ultrasonically cleaned in acetone for 5 min, rinsed in deionized water, etched in a 8.33 vol % HNO_3 and 0.075 vol % HF bath for 12 min, neutralized in a basic solution containing 10 mM NH_4Cl for 20 min, rinsed in deionized water and dried in ambient atmosphere at 50 °C.

The fibres were sifted into intertwined mats from which sheets 120 mm in length, 60 mm in width and 2.3 mm in thickness were pressed. The volumetric density of the fibres was $12 \pm 2\%$. Fig. 1 is a scanning electron microscopy (SEM) micrograph demonstrating the open pore structure of the samples.

To improve the coherence of the mats, these sheets were vacuum-sintered at 975 °C for 30 min at 1.3×10^{-4} Pa and furnace-cooled. After sintering, disc-shaped samples 16 mm in diameter were punched from the sheets, cleaned with the acetone and deionized water treatment described above, passivated in 40 vol % HNO_3 at 50 °C for 20 min, cleaned in deionized water at 50 °C for 5 min and thoroughly rinsed with deionized water at room temperature [23]. These passivated samples were sterilized using ethylene oxide gas.

2.3. Sample characterization

The samples were characterized by weight, specific surface area and surface composition before immersion. One sample from each fabrication batch, six in total, was used to measure specific surface area (Micromeritics, Norcross, Georgia) by the Brunauer–Emmett–Teller (BET) technique [24]. All samples were analysed during the same run to minimize equipment-dependent variance of the specific surface area measurement.

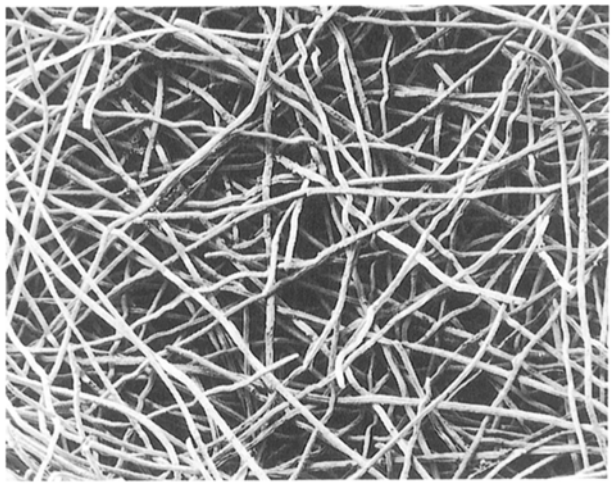

Figure 1 SEM micrograph of a titanium fibre sample (× 13).

The surface composition and oxide stoichiometry of both immersed and non-immersed samples were characterized by Auger electron spectroscopy (AES). AES analyses were performed on a PHI Multiprobe 600 (Perkin–Elmer, Physical Electronics Division, Eden Prairie, Minnesota) equipped with a scanning electron microscope (SEM). Survey spectra were recorded for all samples in the kinetic energy range 10–600 eV. High-resolution surveys of the 90–300 eV region were performed to detect the incorporation of solution electrolytes (Ca, Cl, K, S and P) into the surface. A TiO_2 (rutile) single crystal (Atomergic Chemetals Corporation, Farmingdale, New York) was used to calibrate the peak positions and intensity amplitudes for oxygen (512 eV) and titanium (387 eV) peaks [25]. The wt % of each element was determined from the peak intensity in the differential distribution spectra. The peak-to-peak intensity data were divided by the appropriate elemental sensitivity factor [26] and normalized to 100%. The wt % data are dependent on the accuracy of the reference elemental sensitivity factors, and are considered reliable within 10%.

2.4. Immersion protocol

All liquid-contacting surfaces were cleaned by a standardized acid washing procedure, dried under a class 100 laminar flow hood and gas-sterilized by exposure to ethylene oxide (130 °C, 2 h, 88% air–12% EtO_2).

The solutions were mixed in acid washed plasticware, then sterilized by filtration through a 0.22 μm filter (Millipore Corporation, Bedford, Massachusetts). Before use, the filter assembly was excessively flushed with 0.6 M HNO_3 and thoroughly rinsed with deionized water. The solutions were collected and stored in the sterile acid-washed plasticware until the experiment was initiated.

Six to eight fibre samples were immersed in each test solution for various durations between 70 and 5000 h (208 days). The specimens were placed in 30 ml SIE and EDTA/SIE, and 25 ml serum/SIE contained in polystyrene culture dishes. The lower volume of serum/SIE used was due to the difficulty in collecting large volumes of human serum. The culture dishes were covered with lids that permitted gas exchange and were placed into an incubator maintained at 37 °C, 10% O_2–5% CO_2 and 97 ± 3% relative humidity. Sterile techniques were maintained throughout the experiment. Control groups consisted of polystyrene culture dishes with an identical volume of test solution, but without specimens.

Every 3 days the trays holding the samples were shaken so that the fluid in the inner pore space was displaced, avoiding large concentration gradients from forming. The samples were not agitated more frequently since their low fibre volumetric density allowed them to slide when shaken automatically, thus introducing a component of wear into the experiment, which was undesirable. Evaporation of test solutions was compensated by the addition of sterile deionized water.

Upon expiration of the selected immersion times, the sample group was removed from the incubator and the solution was collected in acid washed polypropylene vials. The vials were capped with a screw lid, wrapped with wax film and frozen until the time of electrothermal atomic absorption spectroscopy (EAAS) analysis. For the control groups a 0.35 ml aliquot of solution was withdrawn at the same time as the sample group, and was stored in a similar manner.

2.5. Titanium concentration in solution

The titanium content in each solution was measured in triplicate by EAAS, and from these data the dissolution kinetics were determined. The absolute dissolution data were normalized by the sample surface area, which was calculated from the specific surface area and weight data. Unique programs that heated liquid samples through a sequence of time and temperature profiles were used to separate the matrix from the analyte. These programs were matrix specific, so the heating phases had to be optimized to minimize the limit of detection. The details of the actual programs used for titanium in SIE, serum/SIE and EDTA/SIE are given in Appendix A. The details of the statistical methods have been described previously [18].

3. Results

3.1. Starting material characterization

An AES survey spectrum for an acid-etched sample is shown in Fig. 2. Due to peak overlap, the N peak was not distinguished from the Ti peak with a kinetic energy range of 372–392 eV. As expected Ti, O and C were detected on the surface. Contaminants other than C included Fe, Ca, Cl, S and Si. This suggested that the acid etching did not completely remove contaminants from the surface. AES surveys collected during each stage of the chemical treatment indicated that after the passivation treatment the contaminants were reduced (Fig. 3). Table II shows the chemical composition of the surface for each stage of the treatment, fibres immersed into EDTA/SIE, and bulk analysis for the fibres and grade 1 titanium. It follows from this table that Fe is eliminated from the surface

TABLE II Surface composition of titanium fibres during various stages of fabrication[a], after immersion in EDTA/SIE and bulk material analysis of grade 1 titanium and titanium fibres after acid etching (see text for definition of treatments)

Treatment	Content (wt %)					
	C	Ti	O	Fe	S	Other
Surface analysis						
AE	14.4	56.9	20.8	5.6	< 0.5	Si, Cl, Ca
AE & S	18.9	47.3	20.6	5.3	1.6	Si, Cl, Ca
AE, S, P & GS	8.1	65.3	25.2	< 0.5	< 0.5	
Immersed EDTA/SIE	15.3	57.4	25.1	< 0.5	0.7	P
Bulk analysis						
Fibre (bulk)	< 0.08	> 99.7		0.15		N, H, O
Grade 1 titanium (bulk) [40]	0.10	> 99.5	0.18	0.20		N, H

[a] AE, Acid-etched; S, sintered; P, passivated; GS, gas-sterilized.

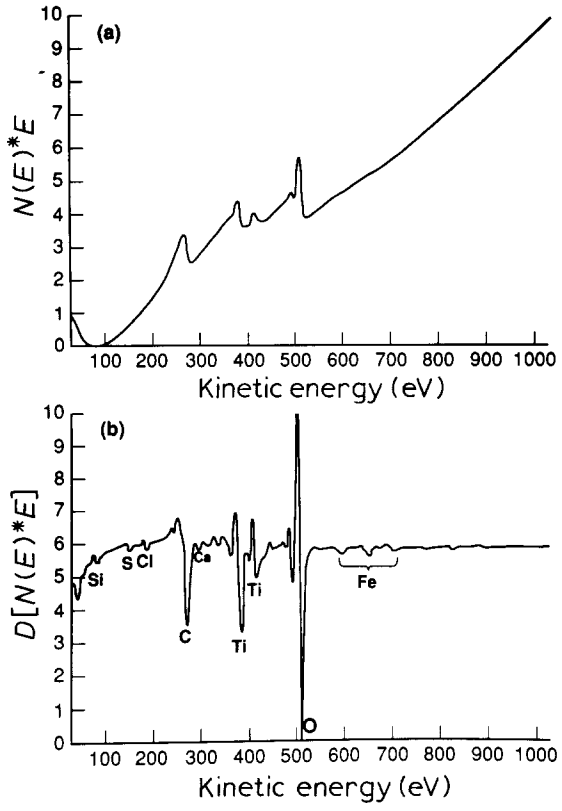

Figure 2 AES survey spectra of an acid-etched sample. The abscissa represents the kinetic energy of the Auger electrons and the ordinate, in arbitrary units, is the peak amplitude. (a) AES data [$N(E)*E$ mode], and (b) AES data processed by a five-point differentiation and an 11-point smoothing routine. The elements present are identified by the negative excursion of the peaks present.

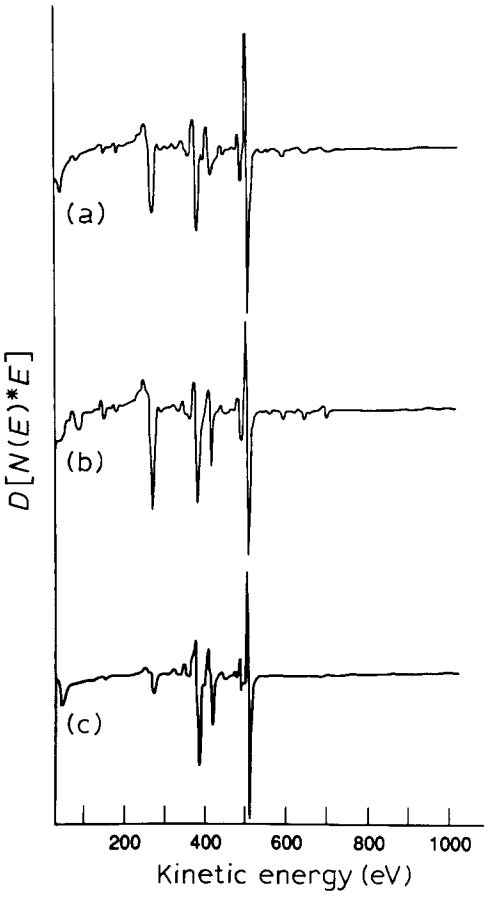

Figure 3 AES survey spectra for various treatments. (a) AE, (b) AE & S and (c) AE, S, P & GS. AE, Acid-etched; S, sintered; P, passivated; and GS, ethylene oxide gas-sterilized.

of the material after the complete chemical processing. Confirmation that the passivation treatment removed the contaminants from the troughs of the fibres is demonstrated in Fig. 4, where the differential Auger electron distribution for a fibre at two distinct points and the corresponding SEM image are shown. The spectra for points 1 and 2 indicate that the contaminants, including Fe, have been uniformly removed from the surface.

The oxide stoichiometry was determined from peak intensity ratios of the O $KL_{2,3}L_{2,3}$ (511–512 eV) and Ti $L_{2,3}M_{2,3}M_{2,3}$ (383–387 eV) Auger transitions measured from the survey spectra [27–29]. The Ti $L_{2,3}M_{2,3}M_{2,3}$ peak was chosen since its line shape and amplitude are consistent for different titanium oxides [29]. In Table III the O/Ti peak intensity ratios for a TiO_2 single crystal (rutile) calibration standard and a non-immersed sample are given. Erratic surface stoichiometry was observed for between- and within-treatment samples. On the completely processed fibres an oxygen-deficient oxide, TiO_{2-x}, inhomogeneously covered the surface. This oxide was interspersed with regions of stoichiometric oxide, TiO_2. This is reflected in the lower O/Ti ratio and the larger associated standard deviations for the fibre measurements compared with that of the TiO_2 single crystal.

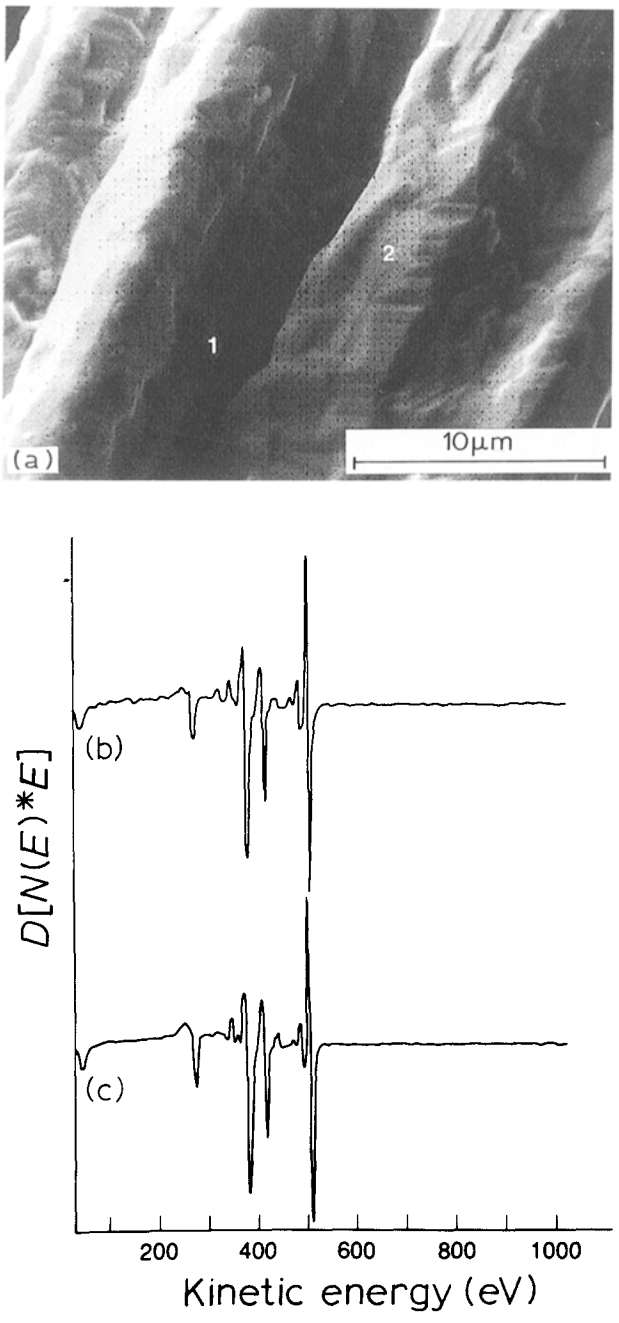

Figure 4 Analysis of a treated (AE, S & P) fibre at specific locations (a) SEM micrograph of the fibre and corresponding AES differential distribution spectra for (b) point 1, in the trough and (c) point 2 AE, Acid-etched, S, sintered, P, passivated; and GS, ethylene oxide gas-sterilized

TABLE III AES intensity ratio of O/Ti for selected samples. The fibres were acid-etched, sintered, passivated and gas-sterilized (AE, S, P & GS) before immersion (means ± standard deviation of repeated measurements)

Sample	O/Ti
TiO_2 single crystal	2.14 ± 0.01
Ti fibre: AE, S, P& GS	1.86 ± 0.25
Ti fibre: immersed in EDTA/SIE	2.11 ± 0.08

TABLE IV Specific surface area of the titanium felt samples as measured by the BET technique (means ± estimated standard deviation of the measurement)

Sample batch	Weight (g)	Specific surface area ($cm^2 g^{-1}$)
1	1.262	355 ± 7
2	1.258	803 ± 4
3	1.237	959 ± 7
4	1.277	238 ± 6
5	1.268	337 ± 7
6	1.224	286 ± 2

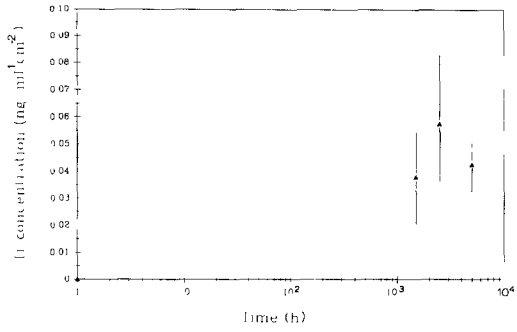

Figure 5 Normalized passive dissolution kinetics for titanium immersed in SIE. The line indicates the limit of detection of titanium in SIE. The error bars indicate the standard deviation of the population mean, including the error associated with the analytical chemical measurement.

The results for the BET determinations are given in Table IV, along with the weight of material used for the analysis.

3.2. Passive dissolution kinetics

Titanium was not detected in any of the control solutions. The results for immersion in SIE are shown semilogarithmically in Fig. 5. The ordinate represents the normalized concentration of titanium, i.e. the Ti concentration divided by the sample surface area. The concentration of titanium in SIE was detectable only at the later three time periods. Thus, even with state-of-the-art detection limits the passive dissolution of titanium in an electrolyte solution is exceedingly low and not detectable at the early time periods of immersion. There was no clear trend with respect to these data and a one-way analysis of variance (ANOVA), for time (controlled variable) and concentration showed these points not to be statistically different at the $P < 0.05$ level. The maximum concentration of titanium released was less than the solubility limit of TiO_2, so the dissolution reaction did not reach equilibrium and the data must represent exceptionally slow kinetics.

The results for samples immersed in serum/SIE were drastically different and are first represented in Fig. 6a. The dissolution rate is shown to decrease with increasing immersion time. A one-way ANOVA for time and concentration indicated a time-dependent variation of the dissolution ($P < 0.0001$). A Student–Newman–Keuls *post hoc* test [30] was used to identify which time periods were statistically different. Although a difference among the latter three time periods was not observed, these periods were significantly different from the others. This suggested that

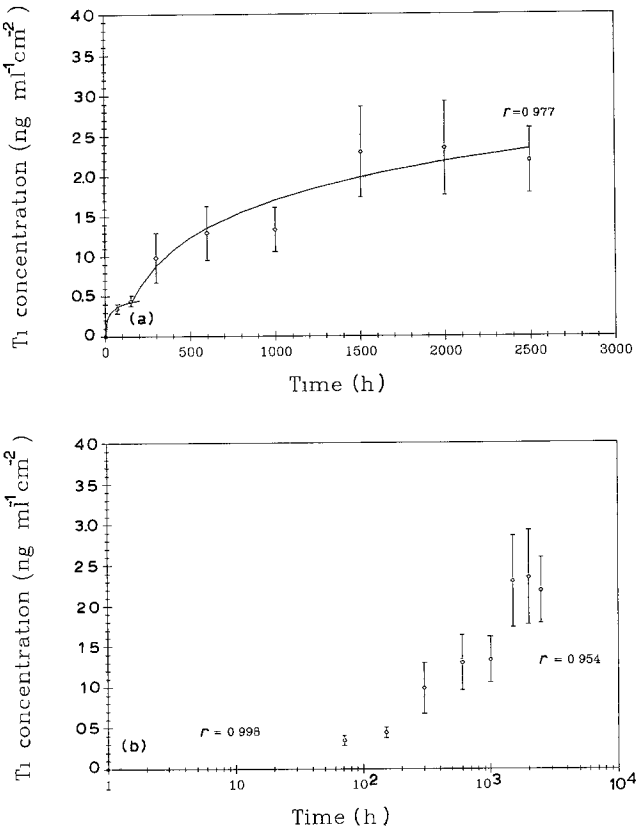

Figure 6 Normalized passive dissolution kinetics for titanium immersed in serum/SIE. (a) Data empirically fitted with two-phase logarithmic (full curve) and power-law relationships (dotted curve), and (b) a semilogarithmic plot of the data, demonstrating the two-phase logarithm relationship The correlation coefficient for the least-squares fit of the linear functions are given. The error bars indicate the standard deviation of the population mean, including the error associated with the analytical chemical measurement.

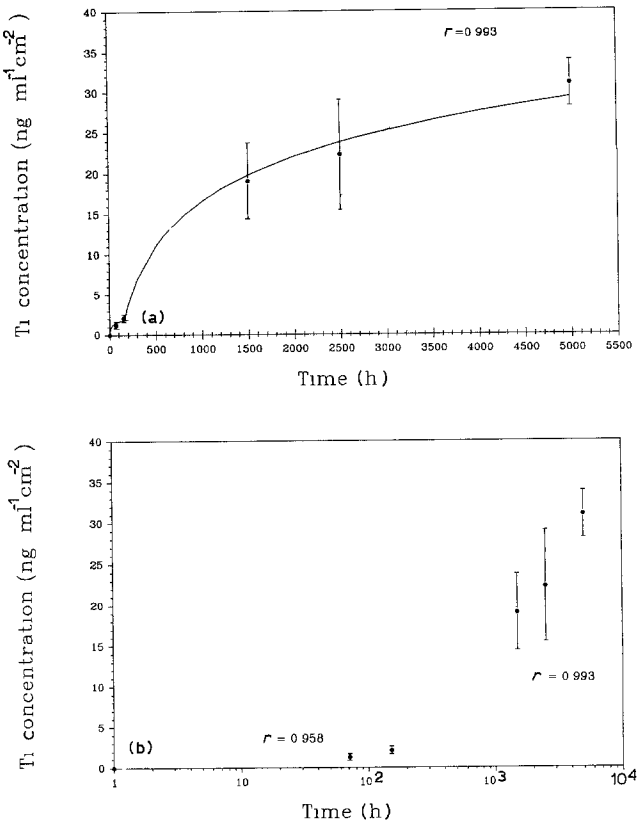

Figure 7 Normalized passive dissolution kinetics for titanium immersed in EDTA/SIE. (a) Real-time data empirically fitted with two-phase logarithmic (full curve) and power-law relationships (dotted curve), (b) a semilogarithmic plot of the data, demonstrating the two-phase logarithm relationship The correlation coefficient for the least-squares fit of the linear functions are given. The error bars indicate the standard deviation of the population mean, including the error associated with the analytical chemical measurement.

either equilibrium was reached, the activities of the biomolecules in solution were depleted, or the scatter in the data masked an increasing trend.

In Fig. 6b the data are represented semilogarithmically. The dissolution pattern was empirically modelled by a two-phase logarithmic relationship. Each phase was fitted with a linear function by the least-squares method [31]. This is shown in the figure with a transition between phases in the 200–300 h range. These data indicate that dissolution occurred in two phases, where the initial phase proceeded at a higher rate. The two-phase logarithm relationship was then fitted to the linear graph, along with the best power-law model. The power-law model was obtained by plotting the data on log–log coordinates and applying the least-squares method to obtain the optimum function: the correlation coefficient is indicated in Fig. 6a.

As shown in Fig. 7, the passive dissolution kinetics in EDTA/SIE demonstrated a pattern similar to the serum/SIE solution. There was a decrease in the dissolution rate with time, and a two-phase logarithmic model fitted the data well, with a similar transition between phases at around 200–300 h. The release rate did not reach equilibrium after 5000 h immersion, which was confirmed by one-way ANOVA and Student–Newman–Keuls statistical tests which showed the latter point to be statistically different from the other points ($P < 0.05$). The power-law relationship was also fitted to these data in Fig. 7a. All numerical values for the released concentrations are given in Appendix B.

3.3. Post-immersion surface characterization

The AES O/Ti intensity ratio for a fibre immersed in EDTA/SIE is shown in Table III. After immersion in EDTA/SIE the oxide appeared homogeneous and nearly stoichiometric, but P and S were also detected. This suggests that the oxide healed to a near TiO_2 composition during immersion and incorporated components of the electrolyte solution.

The samples immersed in serum/SIE were covered by a film containing C, N and O. The thickness of the film suppressed the Ti peaks and precluded further AES analysis of the oxide. Analysis of a similar overlayer on titanium thin films with X-ray photoelectron spectroscopy suggested that the film was proteinaceous; possibly lipoprotein- or glycolipid-based [32].

4. Discussion

The solution ligands affected the passive dissolution kinetics of titanium. Comparison of the data for titanium immersed in SIE, serum/SIE and EDTA/SIE

indicated there was a difference in the magnitude of dissolution for each solution. A two-way ANOVA of the data for each solution at equivalent immersion times showed that a significant difference in dissolution rate occurred ($P < 0.0001$). The order of decreasing rate, EDTA/SIE > serum/SIE > SIE, has important implications with respect to the effect of biomolecules. The difference in the magnitude of titanium released from SIE and serum/SIE conclusively demonstrates that organometallic interactions amplify the passive dissolution kinetics. This observation is in contrast to those made by Clark and Williams [10], Hurlen and Wilhelmsen [33] and Solar *et al.* [34], but in agreement with those of Kelly [35], Abd El Kader *et al.* [14] and Williams *et al.* [12] who demonstrated that the constituents of the solution influence the corrosion of titanium.

These observations may be interpreted by considering the interaction of the final corrosion product with ligands in solution. At the pH of the current experiments the final corrosion product is not Ti^{4+} (aq) but a titanium hydroxyl complex consistent with the hydrolysis reaction, e.g. $Ti(OH)_4$, reaction [36, 37]

$$TiO_2 + 2H_2O \rightleftharpoons Ti(OH)_4 \quad (1)$$

The $Ti(OH)_4$ is in equilibrium with $Ti(OH)_3^+$ and OH^- as described by

$$Ti(OH)_4 \rightleftharpoons Ti(OH)_3^+ + OH^- \quad (2)$$

In the presence of EDTA and serum biomolecules the dissociated ion can form a molecular complex, driving Reaction 2 towards further dissociation. This enhances the reaction rate for dissolution, since the final corrosion products are constantly removed. This assumption is logical in view of the rapidity and strength of the titanium–EDTA chelation reaction [18, 19]. In the SIE solution there is no enhancement because neither EDTA nor serum proteins, to which the same effect is ascribed, are present. The solution-mediated reactions

$$Ti(OH)_3^+ + H_2Y^{2-} \rightleftharpoons Ti(OH)_3HY^{2-} + H^+$$

$$H_4Y = \text{EDTA} \quad (3)$$

$$Ti(OH)_3^+ + B^{n-} \rightleftharpoons Ti(OH)_3B^{(1-n)}$$

$$B = \text{biomolecules} \quad (4)$$

show the molecular complexes formed between the dissolution reaction products, EDTA and serum biomolecules.

These reactions did not achieve equilibrium in our system because the concentrations of EDTA and serum proteins were excessively greater than the concentration of titanium. For example, the maximum conversion of the EDTA molecule assuming irreversible binding with titanium (measured concentration) after 5000 h immersion is <1%. However, the dissolution kinetics observed indicate that saturation within the surface boundary layer occurs. For titanium thin films similar release rates have been modelled by Fickian kinetics [38].

The interactions of EDTA and serum biomolecules enhance the passive dissolution kinetics as described above, but to a different degree. This is probably due to the concentration of EDTA used to model the interaction of serum proteins. The concentration of EDTA used was based on the assumption that all proteins in serum are active in complexing the dissolution products. In view of the present data it appears that not all serum proteins are involved in the binding, and that the reaction rate constants of those involved are not the same. Furthermore, molecular species other than serum proteins may be involved. An exact model of the dissolution reaction rates between serum biomolecules and titanium requires a knowledge of the reaction rate constants for all of the complexing species.

Beyond the actual kinetics, one can focus on the reaction pathway. It then appears that EDTA and serum proteins enhance passive dissolution by a similar mechanism. Even though the magnitude of release was different for the serum/SIE and the EDTA/SIE solutions, the same pattern of release was established. This is clearly demonstrated by a dual ordinate plot of the data for each solution (Fig. 8). Within experimental error these data indicate that the dissolution reaction order is the same for both solutions.

The two-phase logarithmic representation of the dissolution data is preferred based on physical considerations. Before immersion, AES analyses of the fibres showed the oxide to be an excess cation oxide, i.e. non-stoichiometric TiO_{2-x}. During immersion the oxide changed to nearly stoichiometric TiO_2. Based on these findings and the dissolution kinetics, it is proposed that the first phase of dissolution ($t < 300$ h) is dominated by equilibration of the oxide with the solution, and the second phase of dissolution ($t > 300$ h) is dominated by another mechanism, mass diffusion within the concentration boundary layer [38].

It is difficult to assess the efficacy of the EDTA/SIE and serum/SIE solutions to model the *in vivo* environment. In light of the large difference in the concentration of titanium measured *in vivo* [1–8] and the current results *in vitro*, the *in vitro* results must be interpreted as the minimum amount of release possible with a well-prepared and controlled material. With this in mind, EDTA/SIE can serve as a model solution for serum/SIE in future experiments, particularly with the samples of low surface area that are necessary for

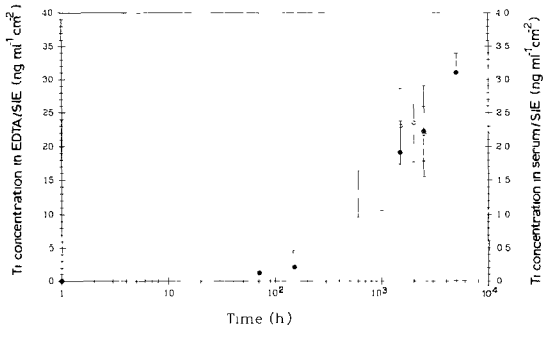

Figure 8 A dual ordinate plot comparing the passive dissolution kinetics for titanium in (◇) serum/SIE and (●) EDTA: semi-logarithmic plot

experiments addressing the mechanisms of dissolution. Possible reasons for the variations in the magnitude of titanium released *in vivo* include oxides with different physical chemistries, chemical reactions due to inflammation and trauma that produce additional biomolecules *in vivo* [39], and the breaking of formed oxide needles [11, 34] imparting a particulate form of titanium.

5. Conclusions

Solution ligands such as serum molecules and EDTA enhance the dissolution of titanium, following a similar reaction order. Thus, EDTA is a valuable reagent for modelling the dissolution kinetics of more complex solutions containing serum. Concomitant with the dissolution reactions, the originally cation excess oxide (TiO_{2-x}) equilibrated with the solution to nearly ideal stoichiometry. A two-phase kinetic model was proposed to accommodate both dissolution and oxide equilibration, where each phase was dominated by a distinct mechanism.

Appendix A

EAAS measurements

The instrument was calibrated by measuring the absorbance signal of a known titanium concentration standard. From a series of concentration standards, an absorbance versus concentration calibration curve was established and used to calculate the concentration of the unknown samples. Since EAAS is subject to matrix background and chemical interference, the most accurate calibration standards consist of identical matrices as the samples. For SIE and EDTA/SIE solutions this was achieved; however, matching standards was not possible for serum/SIE analyses. The methods of the analysis are given in detail elsewhere [42]. Briefly, EDTA/SIE was used as a matrix modifier to prevent precipitation of the titanium corrosion products in the SIE; a 1:1 dilution was used for both the standards and samples. Serum/SIE was analysed by using 0.03 M HNO_3 standards diluted with two parts 0.03 M HNO_3 + 0.375% Tritron X-100 (Alkylaryl Polyether Alcohol, J.T. Baker) [43]. The 2:1 dilution gave a final concentration of Tritron X-100 equivalent to 0.25%. The addition of Tritron X-100 detergent to the serum/SIE aided in spreading the sample aliquot over the graphite tube, which promoted even and reproducible drying, and eliminated the build-up of ash in the tube. This improved the accuracy and repeatability of the measurement. The use of HNO_3 calibration standards was confirmed by the method of additions. The two calibration curves were statistically tested against the null hypothesis that there was a significant difference between each. The hypothesis was rejected ($P < 0.01$), and the dilute HNO_3 was used as the calibration standard for serum/SIE.

TABLE V EAAS detection limits (means ± standard deviation) in SIE, EDTA/SIE and serum/SIE

Solution	Detection limit (ng Ti ml^{-1})
SIE	0.9 ± 0.1
EDTA/SIE	0.7 ± 0.01
Serum/SIE	3.0 ± 0.6 (1.0 ± 0.2)

The detection limits, in ng titanium ml^{-1}, for each solution are given in Table V. The value in parentheses is the detection limit of the diluted serum/SIE sample matrix. The reported value was corrected for the dilution factor of 3. Detection limits at these concentrations can be achieved only through stringent control of contamination from extraneous sources. This requires the use of distilled deionized water, ultrapure reagents and ultraclean plasticware for the preparation of all samples and standards [44–46].

EAAS programs

The characteristics of the EAAS analyses for titanium in SIE, EDTA/SIE and serum/SIE are given below. The following furnace programs should be considered only as a general guideline, since operational parameters can be altered by seasonal fluctuations in the cooling water temperature. The program for each solution varied due to the difference in matrix composition, but the instrumental parameters for titanium were the same for each solution.

Titanium EAAS parameters

Spectral wavelength: 365.3 nm.
Spectral width: 0.2 nm low.
Ti hollow cathode lamp current: 38 mA.
Background correction: W lamp.

SIE

Peak area measurement: 8 s read time.
Determination off tube wall.
Absorbance/concentration: 0.05 A s(10 ng Ti $ml^{-1})^{-1}$.
Standards matrix: 1:1 (v/v) SIE to 8.0 mM EDTA/SIE.
Sample Matrix: 1:1 (v/v) SIE to 8.0 mM EDTA/SIE.

Step	Drying				Charring	Atomization	Cool	Cleaning
	1	2	3	4	5	6	7	8
Temperature (°C)	80	100	120	350	1500	2700	20	2800
Ramp time (s)	1	40	15	15	20	0	1	2
Hold time (s)	3	20	5	5	20	8	3	3
Baseline (s)					24			

EDTA/SIE

Peak area measurement: 8 s read time.
Determination off tube wall.
Absorbance/concentration: 0.05 A s(10 ng Ti ml^{-1})$^{-1}$.
Standards matrix: 8.0 mM EDTA/SIE.
Sample matrix: 8.0 mM EDTA/SIE.

Step	Drying				Charring	Atomization	Cool	Cleaning
	1	2	3	4	5	6	7	8
Temperature (°C)	80	100	120	350	1500	2700	20	2800
Ramp time (s)	1	40	15	15	20	0	1	2
Hold time (s)	3	20	5	5	20	8	3	3
Baseline (s)					24			

Serum/SIE

Peak area measurement: 8 s read time.
Determination off tube wall.
Absorbance/concentration: 0.04 A s(10 ng Ti ml^{-1})$^{-1}$.
Standards matrix: 0.03 M HNO_3.
Sample matrix: 1:2 (v/v) serum/SIE to 0.03 M HNO_3 + 0.375% Tritron X-100.

Step	Drying				Charring	Atomization	Cool	Cleaning
	1	2	3	4	5	6	7	8
Temperature (°C)	80	100	120	400	1600	2700	20	2800
Ramp time (s)	1	40	15	10	20	0	1	2
Hold time (s)	3	40	5	5	20	8	5	3
Baseline (s)					26			

Appendix B
EAAS data

Normalized concentration of titanium in various solutions Mean ± standard deviation and number of samples (*n*)

Solution	Time of immersion (h)	Ti concentration (ng ml^{-1} cm^{-2})	*n*
SIE	70–1000	ND	
SIE	1500	0.038 ± 0.017	6
SIE	2500	0.058 ± 0.025	6
SIE	5000	0 043 ± 0 025	4
Serum/SIE	70	0.347 ± 0.062	6
Serum/SIE	150	0.443 ± 0.065	5
Serum/SIE	300	0.958 ± 0 314	6
Serum/SIE	600	1.30 ± 0 338	6
Serum/SIE	1000	1.34 ± 0 278	6
Serum/SIE	1500	2.30 ± 0.565	6
Serum/SIE	2000	2 35 ± 0.582	6
Serum/SIE	2500	2.19 ± 0.406	4
EDTA/SIE	70	1.26 ± 0.436	7
EDTA/SIE	150	2.11 ± 0 489	7
EDTA/SIE	1500	19.1 ± 4 68	6
EDTA/SIE	2500	22.3 ± 6 81	6
EDTA/SIE	5000	31 0 ± 2.89	8

ND, Not detectable.

References

1 G MEACHIM and D F WILLIAMS, *J Biomed. Mater. Res* **7** (1973) 555.
2. D F WILLIAMS and G MEACHIM, *J. Biomed. Mater Res Symp* **5** (1974) 1
3 P G LAING, A B FERGUSON and E S HODGE, *J Bone Joint Surg.* **41A** (1959) 737
4 A B FERGUSON, Y AKAHOSHI, P. G LAING and E S HODGE, *ibid.* **44A** (1962) 323.
5. *Idem, ibid.* **44A** (1962) 317
6. G J WILLEMS, R A PALMANS, J COLARD and P DUCHEYNE, *Analysis* **12** (1984) 443.
7. P DUCHEYNE, G WILLEMS, M MARTENS and J HELSEN, *J Biomed. Mater Res.* **18** (1984) 293
8. J L WOODMAN, J J JACOBS, J O GALANTE and R M URBAN, *J Orthopaed Res.* **1** (1984) 421.
9 J C KELLER, F A YOUNG and B HANSEL, *Dent Mater.* 1(2) (1985) 41
10. G C F CLARK and D F WILLIAMS, *J. Biomed Mater. Res.* **16** (1982) 125.
11. R J SOLAR, S R POLLACK and E KOROSTOFF, in "Corrosion and Degradation of Implant Materials", ASTM STP 684, edited by B C. Syrett and A. Acharya (American Society for Testing and Materials, Eastern Maryland. 1979) p 161
12 R L WILLIAMS, S A BROWN and K MERRITT, *Biomaterials* **9** (1988) 181.
13 A C. FRAKER, A W RUFF and M P YEAGER in "Titanium Science and Technology", Vol 4 (Plenum Press, New York, 1973) p. 2447
14 J. M ABD EL KADER, F M. ABD WAHAB, H A EL SHAYEB and M G. A KHEDR, *Brit. Corros. J* **16** (1981) 111.
15 P DUCHEYNE and K E HEALY, in "Surface Characterization of Biomaterials", edited by B D. Ratner (Elsevier Science, Amsterdam, 1988) p 175
16. P DUCHEYNE, M MARTENS, W COLEN and P DELPORT, *Trans. Soc. Biomater.* **7** (1984) 185
17. H LONSMANN POULSEN, *Scand J. Clin. Lab. Invest* **34** (1974) 119
18 P DUCHEYNE and K E HEALY, *J Biomed. Mater Res* **22** (1988) 1137. Errata for this reference: the exponent 1/2 was omitted from the variances, $V(E)$ in equation 4 $[V(E)^{1/2}]$ and $V(\mu)$ in section 6 $[V(\mu)^{1/2}]$.
19. A RINGBOM, "Complexation in Analytical Chemistry" (Krieger, Huntington, New York, 1979)
20 K E HEALY and P DUCHEYNE Unpublished data
21. L C COVINGTON and R W SCHUTZ, in "Industrial Applications of Titanium and Zirconium", ASTM STP 728, edited by E W. Kleefisch (American Society for Testing and Materials, Philadelphia, Pennsylvania, 1981).

22. H B BOMBERGER, in "Industrial Applications of Titanium and Zirconium: Third Conference", Philadelphia, ASTM STP 830, edited by R. T. Webster and C. S. Young (American Society for Testing and Materials, 1984) p. 143.
23 ASTM Standard F86: Standard recommended practice for surface preparation and marking of metallic surgical implants (American Society for Testing and Materials, Philadelphia, Pennsylvania, 1976).
24. S. BRUNAUER, P H EMMETT and E TELLER, *J. Amer. Chem. Soc.* **60** (1938) 309.
25. K E. HEALY and P DUCHEYNE, *J. Colloid Interf. Sci.* **150** (1992) 404.
26. L E. DAVIES, N C MAC DONALD, P. W. PALMBERG, G E RIACH and R E WEBER, "Handbook of Auger Electron Spectroscopy" (Physical Electronics Division, Perkin–Elmer Corporation, Eden Prairie, Minnesota, 1978).
27. H. J. MATHIEU, J. B MATHIEU, D. E Mc CLURE and D LANDOLT, *J. Vacuum Sci. Technol.* **14** (1977) 1023.
28. P B. SMITH and S. L BERNASEK, *Surf. Sci.* **188** (1987) 241.
29. N R ARMSTRONG and R. K. QUINN, *ibid.* **67** (1977) 451
30. G. W SNEDECOR and W G. COCHRAN, "Statistical Methods", 7th Edn. (Iowa State University Press, Ames, Iowa, 1980)
31. J P. HOLMAN and W J GAJDA, JR, "Experimental Methods for Engineers", 3rd Edn. (McGraw-Hill, New York, 1978).
32. K. E HEALY and P. DUCHEYNE, *Biomaterials* **13** (1992) 553.
33. T HURLEN and W. WILHEMSEN, *Electrochim. Acta* **31** (1986) 1139.
34. R J SOLAR, S R. POLLACK and E KOROSTOFF, *J. Biomed. Mater. Res.* **13** (1979) 217.
35. J J KELLY, *Electrochim Acta* **24** (1979) 1273
36. P -A MAEUSLI, P R BLOCH, V. GERET and S G STEINEMANN, in "Biological and Biomechanical Performance of Biomaterials", edited by P. Christel, A. Meunier and A. J. C. Lee (Elsevier Science, Amsterdam, 1986) p. 57
37. C. F BAES and R E MESMER, "The Hydrolysis of Cations" (Wiley, New York, 1976) p. 147
38. K. E HEALY and P DUCHEYNE, *J Biomed. Mater. Res.* **26** (1992) 319.
39. P. TENGVALL, I LUNDSTROM, L SJOQVIST, H ELWING and L. M BJURSTEN, *Biomaterials* **10** (1989) 166.
40. A LEAF and L H NEWBURGH, "Significance of the Body Fluids in Clinical Medicine", 2nd Edn (Thomas, Springfield, Illinois, 1955).
41. ASTM Standard F67-83 (American Society for Testing and Materials, Philadelphia, Pennsylvania, 1976).
42. K. E. HEALY, PhD dissertation, University of Pennsylvania, Philadelphia, Pennsylvania (1990).
43. N. W ALCOCK, *Atomic Spectrosc.* **5** (3) (1984) 78.
44. J. VERSIECK, F. BARBIER, R. CORNELIS and J HOSTE, *Talanta* **29** (1982) 973.
45. J. VERSIECK, *Trace Elements Med.* **1** (1984) 2.
46. R CORNELIS, *J. Radioanalyt. Nucl. Chem.* **112** (1987) 141.

Received 8 May
and accepted 11 June 1992